

Article

A Novel Cu²⁺ Quantitative Detection Nucleic Acid Biosensors Based on DNAzyme and “Blocker” Beacon

Hanyue Zhang ^{1,†}, Kai Dong ^{2,†}, Shuna Xiang ¹, Yingting Lin ¹, Xiaoyan Cha ¹, Ying Shang ^{1,*} and Wentao Xu ^{3,*} 

¹ Faculty of Food Science and Engineering, Kunming University of Science and Technology, Kunming 650500, China

² College of Biological Sciences, China Agricultural University, Beijing 100083, China

³ Key Laboratory of Precision Nutrition and Food Quality, Department of Nutrition and Health, China Agricultural University, Beijing 100083, China

* Correspondence: sy_foodsafety@kust.edu.cn (Y.S.); xuwentao@cau.edu.cn (W.X.); Tel.: +86-871-6592-0216 (Y.S.)

† These authors contributed equally to this work.

Abstract: In this paper, a “turn-off” biosensor for detecting copper (II) ions based on Cu²⁺-dependent DNAzyme and a “blocker” beacon were developed. Upon the copper ion being added, the Cu²⁺-dependent DNAzyme substrate strand was irreversibly cleaved, thereby blocking the occurrence of the ligation reaction and PCR, which inhibited the G-rich sequence from forming the G-quadruplex structure, efficiently reducing the detection signal. This method had the characteristics of strong specificity and high sensitivity compared with the existing method due to the application of ligation-dependent probe signal recognition and amplification procedures. Under the optimized conditions, this method proved to be highly sensitive. The signal decreased as the concentration of copper ions increased, exhibiting a linear calibration from 0.03125 μM to 0.5 μM and a limit of detection of 18.25 nM. Subsequently, the selectivity of this biosensor was verified to be excellent by testing different relevant metal ions. Furthermore, this detection system of copper (II) ions was successfully applied to monitor Cu²⁺ contained in actual water samples, which demonstrated the feasibility of the biosensor.

Keywords: biosensor; Cu²⁺; DNAzyme; ligation; PCR; G-quadruplex



Citation: Zhang, H.; Dong, K.; Xiang, S.; Lin, Y.; Cha, X.; Shang, Y.; Xu, W.

A Novel Cu²⁺ Quantitative Detection Nucleic Acid Biosensors Based on DNAzyme and “Blocker” Beacon.

Foods **2023**, *12*, 1504. <https://doi.org/10.3390/foods12071504>

Academic Editor: Antonello Santini

Received: 23 February 2023

Revised: 23 March 2023

Accepted: 28 March 2023

Published: 3 April 2023



Copyright: © 2023 by the authors. Licensee MDPI, Basel, Switzerland. This article is an open access article distributed under the terms and conditions of the Creative Commons Attribution (CC BY) license (<https://creativecommons.org/licenses/by/4.0/>).

1. Introduction

In the environment, heavy metal ions naturally exist in the atmosphere, oceans, and soils due to geological causes. With the progress of human society, mining and smelting in industrial production activities, the use of heavy metal ion pesticides and cadmium-containing fertilizers in agricultural production activities, waste incineration, and automobile exhaust emissions in daily life activities have made heavy metal pollution increasingly serious [1]. These heavy metal ions enter the water and soil and enter the food chain via plants, animals, and microorganisms. Heavy metal ions are absorbed by plants through their roots, transmitted from stems to other tissues, and then accumulated. For plants themselves, the presence of heavy metal ions affects their own growth [2,3]. Animals need to ingest water and other foods for survival. In this process, heavy metal ions may accumulate in animals. In this way, heavy metal ions in the food chain can be transmitted between various nutritional levels, and bioaccumulation, transformation, and biomagnification will eventually endanger human health [4,5]. The Minamata disease caused by mercury-containing industrial wastewater discharge pollution and the painful Itai-itai disease caused by cadmium rice produced on cadmium-containing water-irrigated farmland are warning us to pay attention to the health problems caused by heavy metal pollution.

Nowadays, more and more people pay attention to heavy metal pollution in food safety. Heavy metal ions are a kind of chemical substance that has obvious toxicity to

organisms [6]. Heavy metal ions may cause kidney damage, lung damage, bone damage, nervous system damage, etc. [7]. The heavy metal ions are difficult to degrade by organisms in nature; however, they are widely distributed and then harmful to the environment and human health [8,9]. The copper ion is one of the most important ones among these heavy metal ions. It is a necessary trace element for human growth, and only a small amount of copper ions is needed to maintain the normal life activities of the human body. However, excessive copper ions will interfere with the normal physiological function of the human body and further endanger human health. For example, the gradual accumulation of copper ions in the liver will cause damage to it, and copper can catalyze the formation of hydroxyl radicals, resulting in DNA damage and increased lipid peroxidation [10]. Therefore, it is significant to detect copper ions effectively and sensitively.

There are many ways to detect copper ions, such as the traditional detection methods based on large instruments, including atomic absorption spectrometry (AAS) [11], gas chromatography (GC), inductively coupled plasma mass spectrometry (ICP-MS), high performance liquid chromatography (HPLC) [12,13], and so on. These methods rely on relevant large-scale equipment, expensive supplies, and standard substances, which have the merits of high sensitivity and good specificity. However, the above methods are also inadequate sometimes because of complex sample preparation, a long detection period, and high costs. Hence, it is difficult to meet the requirements of the modern fast, simple, and high-throughput detection tendency.

In recent years, functional nucleic acids have shown great potential and developed rapidly in the detection of heavy metal ions. It has been applied to the detection of many kinds of heavy metal ions, including Pb^{2+} [14,15], Hg^{2+} [16,17], Ag^+ [18,19], Cu^{2+} [20–22] and UO_2^{2+} [23,24]. The term functional nucleic acid refers to a single-chain DNA fragment with catalytic function that has specific structure recognition capacity and excellent catalytic activity. It includes metal ion-dependent DNazymes, and as a DNA-based biocatalyst, it can carry out many biological and chemical reactions. Refs. [25,26] exhibit catalytic activity only when specific metal ions exist and can cause DNA double-strand fragments to break at specific positions to produce smaller oligonucleotide fragments.

A large number of colorimetric [26–31], electrochemical [32–34], and fluorescent [21, 22,35–44] DNzyme-based biosensors have been designed to determine Cu^{2+} with high sensitivity and selectivity. Compared with electrochemical and fluorescent DNzyme sensors, colorimetric sensor technology does not require the use of more expensive instruments and is low cost, which can achieve fast, sensitive, on-site, and visual inspection. At present, the colorimetric sensor technology based on functional nucleic acid detection of copper ions can be divided into two major categories according to gold nanoparticles and G-quadruplex. Wang established a label-free colorimetric method for the detection of metal ions by combining Cu^{2+} -dependent DNzyme with the color change characteristics of gold nanoparticles after aggregation. Under the cutting action of copper ions, the substrate chain of DNzyme is cut and ssDNA is released. They are adsorbed on gold nanoparticles so that gold nanoparticles cannot aggregate and the system does not change color [45].

G-quadruplex DNzymes have seen rapid development in colorimetric sensor design in the past period of time. The G-quadruplex structure is the secondary structure of DNA.

Hemin is used as a cofactor for many oxidases. When hemin is inserted into the G-quadruplex, the catalytic activity of the compound is enhanced [46,47]. Studies have shown that the G-quadruplex was used as a new type of DNzyme with peroxidase activity, the complexes of which were formed by hemin and can catalyze the oxidation of 2,2'-Azino-bis (3-ethylbenzthiazoline-6-sulfonic acid) (ABTS) to produce the free radical cation $ABTS^+$ in the presence of H_2O_2 , and the absorption signal increases at ~ 419 nm [48,49]. Yin realized the highly sensitive detection of copper ions by combining the Cu^{2+} -dependent DNzyme, substrate, and an HRP-mimicking DNzyme into a unimolecular colorimetric sensor [50]. Zhang used the substrate strand of the DNA-cleaving DNzyme and a G-rich sequence as a stem-loop structure, and in the presence of copper ions, the substrate chain cleavage, which can release the G-rich sequence and subsequently form the G-quadruplex DNzyme,

detected the copper ion [51]. For biosensor detection, there are generally three steps: signal recognition, signal amplification, and signal output. There is no signal amplification process in these methods, which may lead to insufficient detection sensitivity. At the same time, the signal recognition procedure is not stable enough and is easily affected by interference factors, especially the non-target metal ion.

Shang designed a novel single universal primer multiplex ligation-dependent probe amplification (SUP-MLPA) technique [52]. The key principle is that only when the probes are exactly matched with the target template sequence can the two be connected for hybridization and amplification; even if there is a base difference, the amplification cannot be realized, which greatly improves the reaction specificity.

In this study, we designed a label-free DNAzyme-ligation-PCR-based colorimetric biosensor for Cu^{2+} . We combined ligation-dependent probe amplification technology with DNAzyme. Then, the primers for hairpin DNA were designed, which include nucleic acid segments, blockers, and the G-rich sequence, for performing PCR to zip off of the hairpin structure, leading the G-rich sequence to fold to form a G-quadruplex structure. Thus, the formation of G-quadruplex was blocked by the addition of copper ions, resulting in signal reduction and the development of a fast, sensitive, and stable “turn-off” colorimetric detection method.

2. Materials and Methods

2.1. Materials and Reagents

The substrate sequence of Cu^{2+} -dependent DNAzyme (Cu-Sub) and the enzyme sequence of Cu^{2+} -dependent DNAzyme (Cu-Enz) and all primers were synthesized by Shanghai Sangon Co. Ltd. (Shanghai, China). The details of these primers and the nucleotide sequences are listed in Table 1. Ultrapure water used throughout all experiments was purified with a Milli-Q system (resistivity $> 18.0 \text{ M}\Omega \text{ cm}^{-1}$). The used metal salts, including $\text{Al}(\text{NO}_3)_3$, Li_2SO_4 , $\text{Pb}(\text{NO}_3)_2$, $\text{Zn}(\text{NO}_3)_2$, KCl , CaCl_2 , CuCl_2 , FeCl_3 , MgCl_2 , MnCl_2 , NaCl , and FeCl_2 , were bought from the Sigma Chemical Company (St. Louis, MO, USA). Other reagents such as NaOH , H_2O_2 (30%), ABTS, Tris, HCl , hemin, 4-(2-hydroxyethyl) piperazine-1-ethanesulfonic acid (HEPES), sodium ascorbate, dimethyl sulfoxide (DMSO), and Triton X-100 were obtained from Baoxin Biotechnology Co. Ltd. (Kuning, China). All the chemical reagents were of analytical grade. The absorption spectrum of the reaction product was measured and recorded by a SpectraMax M5 plate reader (Molecular Devices, Sunnyvale, Calif.).

Table 1. Synthesized oligonucleotides sequence.

Primer Name	Primer Sequence (5' → 3')	Length	Reference	Product Size (bp)
UP-F	CAGGCGCCGCATTTTTATTGC	21		
UP-R	CGTCGATGACATTTGCCGTAG	22		
ligationP-F	CAGGCGCCGCATTTTTATTGCCCTTCCGCCC TTGGTAAGC	40	This study	
ligationP-R	CGTATTAGAAAGAAGCTTCCCGCCCTACGG CAAATGTCATCGACG	46		86
Cu-Sub	GGCGGGAAAGCTTCTTTCTAATACGGCTTACCA AGGGCGGAAGG	44	[21]	
Cu-Enz	GGTAAGCCTGGGCCTCTTTCTTTTAAGAAAGAAC	35		
Hairpin DNA-1F (H1)	GGGTAGGGCGGGTTGGGTTspacer18AACCCAACCCG CCCTACCCAAACAGGCGCCGCATTTTTATTGC	62	This study	
Hairpin DNA-1R (H2)	GGTAGGGCGGGTTGGGTTspacer18AACCCAACCCGCC CTACCCAAAGTCGATGACATTTGCCGTAG	62		

2.2. Preparation of DNAzyme

To form the Cu^{2+} -dependent DNAzyme, Cu-Sub (10 μM) and Cu-Enz (10 μM) were mixed at a ratio of 1:10 in a 200 μL buffer (1.5 M NaCl, 50 mM HEPES, pH 7.0). The mixture was warmed to 90 $^{\circ}\text{C}$ for 3 min and subsequently cooled naturally at room temperature for 1 h to anneal the DNAzyme. The resultant DNAzymes were stored at 4 $^{\circ}\text{C}$.

2.3. Hybridization and Ligation

The hybridization and ligation reactions were conducted in 500 μL PCR reaction vessels using a thermocycler (Applied Biosystems). The 10 \times Ampligase reaction buffer, 2 U Ampligase (Epicentre, Madison, WI, USA), 1 μL of one of the probes (1 μM), and a 1.5 μL template were used as reaction mixes (5 μL total volume).

The conditions were as follows: the DNA was initially denatured at 95 $^{\circ}\text{C}$ for 3 min, followed by 20 denaturation and ligation cycles at 95 $^{\circ}\text{C}$ for 15 s and 65 $^{\circ}\text{C}$ for 5 min. After ligation, the reaction mixes were heated for 5 min at 98 $^{\circ}\text{C}$ to inactivate the enzyme and then stored in a refrigerator at 4 $^{\circ}\text{C}$.

2.4. PCR Amplification

The reaction mixes used for ligation product amplification were prepared in a 25 μL total volume containing 1 μL of each primer (10 μM), 2.5 μL 10 \times Ex Taq buffer, 2 μL dNTP, 0.2 μL Ex Taq polymerase (TaKaRa Biotechnology Co. Ltd., Dalian, China), a 2 μL template from the ligation mix, and 16.3 μL of ultrapure water. DNA denaturation and polymerase activation at 95 $^{\circ}\text{C}$ for 5 min were followed by 30 amplification cycles at 95 $^{\circ}\text{C}$ for 30 s, 60 $^{\circ}\text{C}$ for 30 s, and 72 $^{\circ}\text{C}$ for 30 s, with a final step of 10 min at 72 $^{\circ}\text{C}$. Finally, the reaction products were then cooled to 4 $^{\circ}\text{C}$.

2.5. Colorimetric Determination of Cu^{2+}

For each experiment, the DNA mixture (100 μL) containing 85 μL of ultrapure water, 10 μL of Cu^{2+} stock solution, 5 μL of DNAzyme, and 5 μL of sodium ascorbate (the final concentration was 5 mM) was sequentially added into a centrifuge tube. After 30 min of reaction at 25 $^{\circ}\text{C}$, 1.5 μL of the above mixture was used as the template for the hybridization and ligation reactions (5 μL total volume). Next, during PCR amplification, the aim is to properly fold to form a large number of G-quadruplexes. Then, 2 μL hemin (final concentration of 2 μM) solution was added into the mixture system, mixed well, and incubated at room temperature for 1 h. Subsequently, 8 μL of ABTS (40 mM), 5 μL of H_2O_2 (20 mM), and 60 μL of buffer (100 mM HEPES, pH 7.0, 0.008% (*v/v*) Triton X-100, and 400 mM NaCl) were added. The final volume of the mixture was 100 μL , and the mixture was transferred into a 96-well microtiter plate. After 5 min, Spectra Max M5 (Molecular Devices, Sunnyvale, Calif.) was used to measure and record the absorbance of the reaction product at 419 nm, and the absorbance was used for subsequent quantitative analysis.

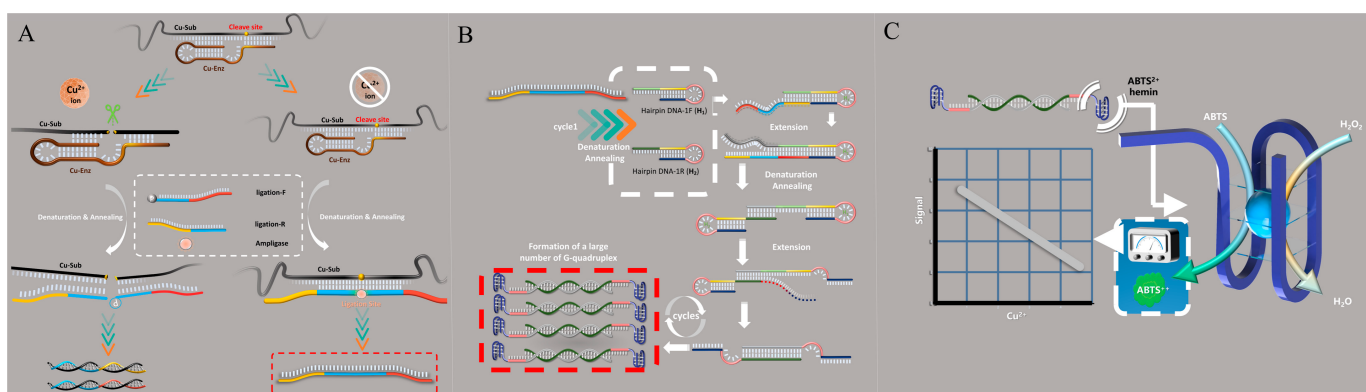
2.6. Analysis of Copper Ion Content in Yunnan Water Samples

Several kinds of water samples (Dianchi Lake and Cuihu Lake) were collected in Kunming, Yunnan Province, P.R. China, and prepared by mixing drinking water with standard Cu^{2+} solution. The concentrations of Cu^{2+} in the water samples were determined by the above-mentioned assay procedures. Conditions: The samples (10 μL) were added to a 100 μL detection system (containing DNAzyme solution and sodium ascorbate). Subsequently, we determined the samples according to the above-mentioned procedures, and the absorbance at 419 nm was recorded. In order to verify the results of this detection method, inductively coupled plasma-mass spectrometry (ICP-MS) was used to detect these water samples.

3. Results and Discussion

3.1. Principle of the Biosensor System

The principle of the DNAzyme-ligation-PCR-based visual “turn-off” colorimetric biosensor for Cu^{2+} is shown in Scheme 1 (Supplementary Materials Figures S1–S3). The system was a combination of three components. Firstly, the Cu^{2+} -dependent DNAzyme was formed by the hybridization between the improved substrate strand and the enzyme strand. Two ligation-F/R probes were designed that were complementary to the substrate strand. Without Cu^{2+} , the substrate strand of the DNAzyme complex was not cleaved. Under the ligase (*Ampligase*) and certain conditions, a ligation-based reaction occurred to produce ligation products. Conversely, if Cu^{2+} presents in the detection system, the substrate strand will be cut into two short chains at the recognition site, and the ligation-based reaction will not happen (Scheme 1A).



Scheme 1. Schematic illustration of the “turn-off” biosensor for the detection of copper (II) ions based on Cu^{2+} -dependent DNAzyme coupled with ligation-dependent probe and PCR amplification technology. (A) Signal recognition of copper ion; (B) Signal amplification; (C) Signal output.

Then, the sequences of hairpin DNA-1F/1R (H_1/H_2) were designed. The H_1 includes a nucleic acid segment complementary to a downstream sequence of ligation products and is connected to a nucleic acid sequence and an oxyethyleneglycol bridge (blocker) to the nucleic acid sequence that is rich in G bases. The H_2 includes a nucleic acid segment complementary to the template, a sequence linked through a blocker tether to the nucleic acid sequence rich in G bases. The blocker is important because the polymerization of the respective templates is always terminated at the blocker. After PCR amplification, the zipping off of the hairpin structure led the G-rich sequence to fold into a G-quadruplex (Scheme 1B).

At last, hemin can bind to the formed G-quadruplex structure to yield a G-quadruplex DNAzyme with catalytic activity, resulting in an increase in the absorbance at 419 nm in the ABTS- H_2O_2 system (Scheme 1C).

While Cu^{2+} was present in the sample, the substrate strand of Cu^{2+} -dependent DNAzyme was cleaved, a ligation-based reaction was not occurring, and it could not form ligation products. Hence, there could not be a large number of active G-quadruplex DNAzymes, resulting in the signal reduction. Thus, a “turn-off” colorimetric detection of copper ions was achieved.

3.2. Verification of the Biosensor System

In order to verify the feasibility of the principle of the biosensor system, the primers UP-F/UP-R were designed. In Figure 1A, without Cu^{2+} , the substrate strand and DNAzyme were present in the system, respectively, and the desired PCR products were analyzed through electrophoresis in a 2.0% agarose gel. While in the presence of Cu^{2+} and DNAzyme at the same time, the substrate strand was cleaved, as shown in Figure 1B. Our results suggested that the principle of the biosensor system is feasible.

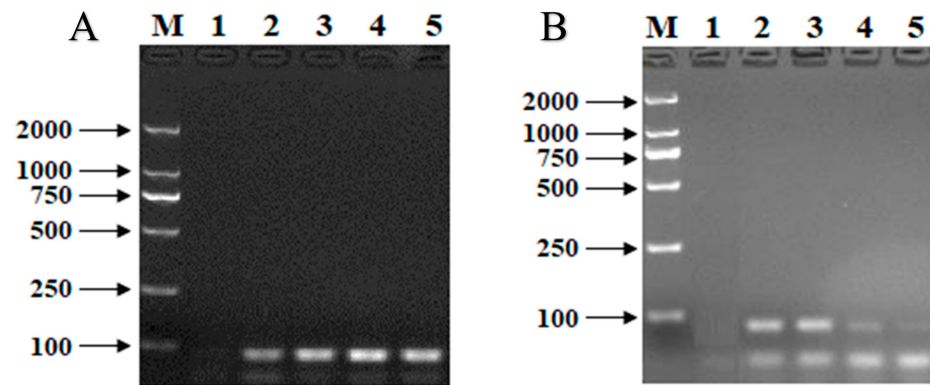


Figure 1. Verification of the biosensor system. (A) Ligation reaction between DNAzyme and ligation-dependent probe. M: DL 2000 (DNA marker); 1: negative control; 2–3: DNAzyme ligation reaction. (B) Cleavage of the substrate chain of DNAzyme Cu^{2+} addition. M: DL 2000 (DNA marker); 1: negative control; 2–3: in the absence of Cu^{2+} ; 4–5: in the presence of Cu^{2+} .

3.3. Optimization of the Biosensor

In order to obtain the best detection system, the optimization of various conditions is necessary. The length of the incubation time of copper ions and DNAzyme has a significant effect on cutting efficiency, and 0.5 h, 1 h, and 1.5 h were set for the reaction time. The result (Figure 2A) shows that when time reaches 0.5 h, it can be completely cut. Thus, considering the time savings, 0.5 h is selected as the optimal cutting time.

The sensitivity depended on the ligation probe concentration; we set the initial concentration of the ligation probe at 10 μM and diluted tenfold from 10 to 0.0001 μM to obtain the amplifying target product proportional to the concentration. (Figure 2B), at 1 μM , amplified bands could be observed most clearly. Therefore, we selected 1 μM as the best probe concentration.

Under different conditions, the cutting efficiency of copper ions is also different. Three kinds of buffer were chosen to perform experiments, including buffer 1 (1.5 M NaCl, 50 mM HEPES, pH 7.0), buffer 2 (100 mM HEPES, pH 7.0, 0.008% (*v/v*) Triton X-100, and 400 mM NaCl), and buffer 3 (ultrapure water). The result is shown in Figure 2C. Under the condition of buffer 3, the change in absorbance (ΔAbs , $\Delta\text{Abs} = \text{Abs}_0 - \text{Abs}$, where Abs_0 represents the absorbance in the absence of copper ions and Abs represents the absorbance in the presence of copper ions) was the biggest. Thus, buffer 3 was used in this study.

The ratio of Cu–Enz and Cu–Sub will affect the amount of substrate cleavage. In order to achieve consistent amplification results, the ratio of Cu–Enz to Cu–Sub was optimized by fixing the substrate chain concentration and changing the amount of Cu–Enz (1:1, 3:1, 5:1, 10:1, and 15:1). Results according to the different ratios of Cu–Enz to Cu–Sub (Figure 2D) at 10:1 and 15:1, the effect is basically the same. Therefore, considering the lower cost, the ratio of Cu–Enz to Cu–Sub was 10:1.

When the concentration of hydrogen peroxide (H_2O_2) is too low, its oxidation ability is not strong; on the contrary, if the concentration of H_2O_2 is too high, it will strengthen the disproportionation. Therefore, it is necessary to optimize the concentration of H_2O_2 . When the final concentration of H_2O_2 reached 1 mM, the effect of the experiment was the best (Figure 2E).

Under different ionic conditions, G-quadruplex, which binds to hemin, showed different catalase activity. The experiments were carried out by selecting six different conditions (buffers 1–6, in Figure 2F). The results (Figure 2F) showed that the best catalytic activity was obtained under the condition of buffer 2. The original measurement data of Figure 2C, 2D, 2E and 2F are shown in Tables S1, S2, S3 and S4 respectively.

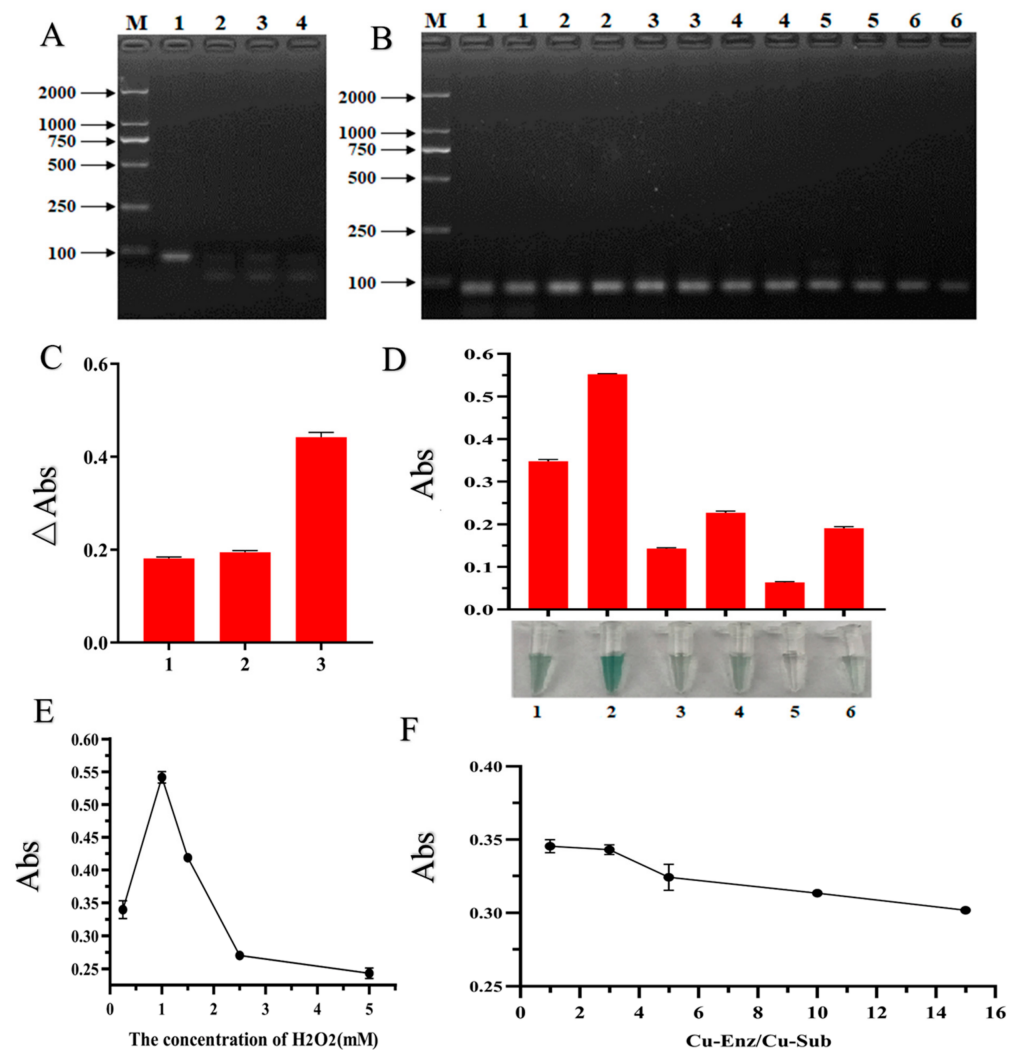


Figure 2. The results of the system optimization. (A) Optimization of cleavage time. M: DL 2000 (DNA Marker); 1: 0 min; 2: 30 min; 3: 60 min; 4: 90 min. (B) Optimization of ligation probe concentration. The concentration of the probes was diluted tenfold from 10 to 0.0001 μM . M: DNA marker DL 2000; 1: 10 μM ; 2: 1 μM ; 3: 0.1 μM ; 4: 0.01 μM ; 5: 0.001 μM ; 6: 0.0001 μM . (C) Optimization of cutting conditions of copper ion. 1: 1.5 M NaCl, 50 mM HEPES, pH 7.0; 2: HEPES 100 mM, pH 7.0, 0.008% (*v/v*) Triton X-100 and 400 mM NaCl; 3: ultrapure water. (D) Optimization of chromogenic ionic conditions. 1: 1.5 M NaCl, 50 mM HEPES, pH 7.0; 2: 100 mM HEPES, pH 7.0, 0.008% (*v/v*) Triton X-100 and 400 mM NaCl; 3: 10 mM Tris-HCl pH 7.4, 10 mM KCl, 100 mM NaCl, 0.002% (*v/v*) TritonX-100; 4: 10 mM Tris-HCl (pH 8.0), 0.002% (*v/v*) TritonX-100, 1.6 mM KCl, 0.8 mM MgCl_2 ; 5: 50 mM NaCl, 10 mM Tris-HCl (pH 7.9), 10 mM DTT, 10 mM MgCl_2 ; 6: ultrapure water. (E) Optimization of the concentration of H_2O_2 . The final concentrations of H_2O_2 are: 0.25 mM, 1 mM, 1.5 mM, 2.5 mM, and 5 mM. (F) Optimization of the ratio of Cu-Enz and Cu-Sub. The ratios from Cu-Enz to Cu-Sub are: 1:1, 1:3, 1:5, 1:10, and 1:15.

3.4. Sensitivity of the Biosensor

Applying the above optimization conditions, the sensitivity of the biosensor was determined by recording the absorption signal after the addition of different concentrations of Cu^{2+} . As shown in Figure 3A, with the increase in the concentration of copper ions, the absorbance signal decreased gradually until reaching a plateau. A linear relationship was observed in Figure 3B; the linear regression equation was $Y = -0.13253X + 0.545$ ($R^2 = 0.994$) over a range of 31.25 nM to 500 nM Cu^{2+} , and the detection limit was determined to be 18.25 nM ($3\sigma/\text{slope}$, where σ is the standard deviation for determining the blank sample),

which represents one of the most sensitive Cu^{2+} determination methods. According to the World Health Organization (WHO), which defined the maximum permitted contamination level of Cu^{2+} in drinking water to be $20 \mu\text{M}$, this detection limit is far below the regulated level. The original measurement data in Figure 3B had shown in Table S5.

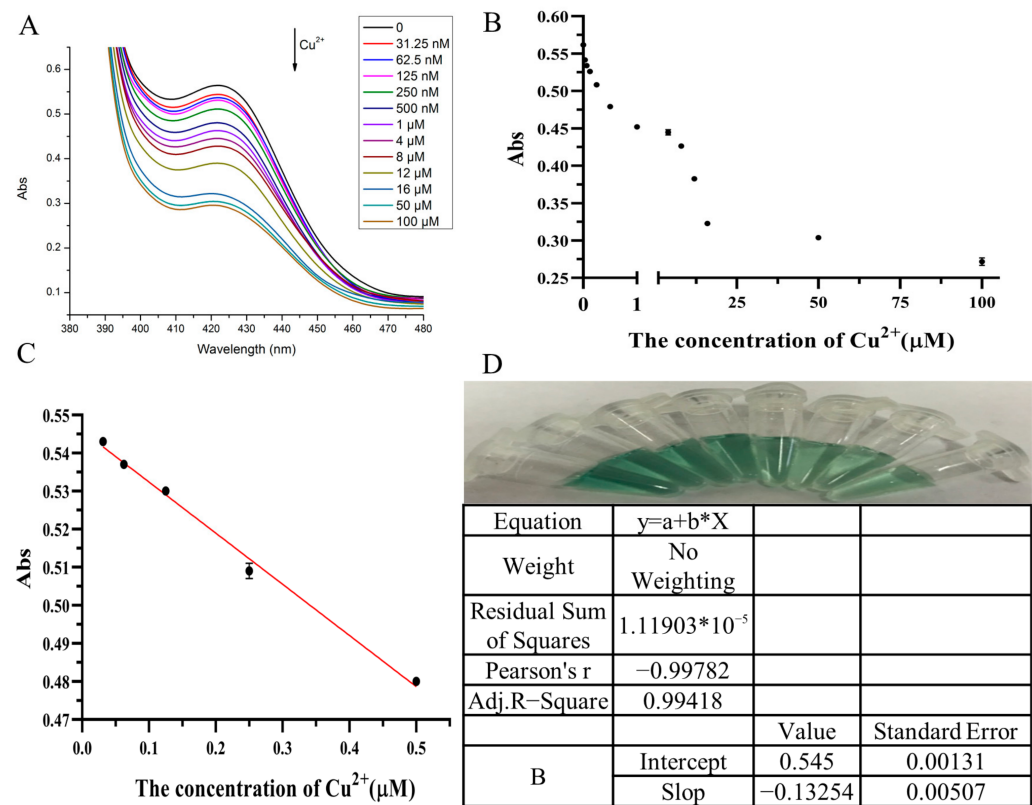


Figure 3. Sensitivity of the Cu^{2+} sensor system. (A) UV-vis absorption spectra change under different Cu^{2+} concentrations. The concentrations of Cu^{2+} are: 0, 31.25 nM, 62.5 nM, 125 nM, 250 nM, 500 nM, 1 μM , 4 μM , 8 μM , 12 μM , 16 μM , 50 μM , and 100 μM . (B) Absorbance ($\lambda = 419 \text{ nm}$) under different Cu^{2+} concentrations. The concentrations of Cu^{2+} are: 0, 31.25 nM, 62.5 nM, 125 nM, 250 nM, 500 nM, 1 μM , 4 μM , 8 μM , 12 μM , 16 μM , 50 μM , and 100 μM . (C) The absorption signals of different Cu^{2+} concentrations at $\lambda = 419 \text{ nm}$. The inset shows that when the concentration of Cu^{2+} is in the range of 31.25 ~ 500 nM, the concentration is linear with the color change. (D) The color of the detection results of different Cu^{2+} concentrations and correlation measurement data.

3.5. Selectivity of the Biosensor

To evaluate the selectivity of the biosensor to Cu^{2+} , different relevant metal ions with a concentration of $10 \mu\text{M}$ were used for detection, including Cu^{2+} , Fe^{3+} , Fe^{2+} , Al^{3+} , Ca^{2+} , Pb^{2+} , Mn^{2+} , Zn^{2+} , Li^{+} , and Mg^{2+} . In Figure 4A,B, in the presence of Cu^{2+} , the change of absorbance (ΔAbs , $\Delta\text{Abs} = \text{Abs}_0 - \text{Abs}$, where Abs_0 represents the absorbance in the absence of metal ions and Abs represents the absorbance in the presence of metal ions) gave a remarkable enhanced absorbance signal and had a noticeable weakening of the color. These results indicated that the biosensor system had good selectivity toward Cu^{2+} . The original measurement data in Figure 4A had shown in Table S6.

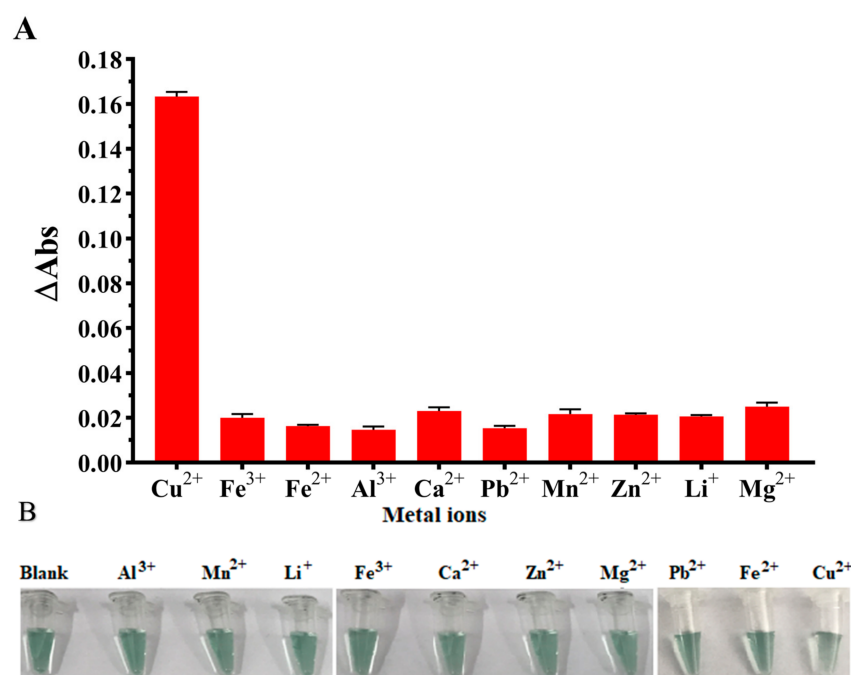


Figure 4. Selectivity of the Cu²⁺ sensor system. (A) the change of absorbance (Δ Abs) of the turn-off sensor after adding different metal ions. (B) The chromogenic results. The final concentrations of the different metal ions are 10 mM.

3.6. Application of the Biosensor

To investigate the practical application and the analytical reliability of the biosensor, combined with the geographical environment, we selected two water samples from Dianchi Lake and Cuihu Lake in Yunnan Province as representative samples. The method developed in this study and a highly sensitive, classical metal ion detection method (inductively coupled plasma-mass spectrometry, ICP-MS) were used for standard addition recovery experiments, and the detection results were compared and analyzed.

In this experiment, the copper ion content of the sample itself was first detected by two methods, and then the copper ion with a concentration of 0.1 μ M was added to the sample for mixing and detection again. The detection values of the two methods were compared, and the recovery rate was calculated to verify the practicability of the detection method in this study. The experimental results are shown in Table 2. The original measurement data in Table 2 had shown in Table S7.

Table 2. Determination of Cu²⁺ in four different water samples using the biosensor and ICP-MS.

	Sample	C1		C2		C3		Recovery (%)
		(μ M)	RSD (%)	(μ M)	RSD (%)	(μ M)	RSD (%)	
This method	Dianchi lake	0.22	4.75	0.1	5.29	0.314	4.21	94
	Cuihu lake	0.179	6.86	0.1	6.24	0.275	4.84	96
ICP-MS	Dianchi lake	0.228	2.33	0.1	2.97	0.318	1.24	90
	Cuihu lake	0.184	2.15	0.1	2.97	0.281	1.23	97

C1: Concentration measured in primary samples. C2: Added copper ion concentration. C3: Concentration of the samples after the addition of copper ions. Rate of recovery = $(C3 - C1)/C2 \times 100\%$. Relative standard deviation (RSD) = standard deviation (SD)/arithmetic mean value (\bar{X}) $\times 100\%$.

For the selection of test samples, this study considered that Dianchi Lake is the largest fresh lake in Yunnan [53], which is located in the enrichment area of phosphorus [54], and it has been listed as one of the three most polluted lakes in China [55]. Cuihu Lake is located in the center of the main urban area of Kunming, with vigorous commercial development [56].

Its social and economic development has made its water pollution increasingly serious. Due to some natural factors, as well as agricultural fertilizer water, industrial wastewater, and the inflow of domestic sewage from surrounding residents, these lakes have eutrophication (water bodies rich in nitrogen, phosphorus, and other substances) [57], and there is a problem of heavy metal ion pollution [58]. Compared with other water sources (such as tap water or rainwater), the composition of the lake sample itself was more complex and had a greater impact on the measurement results of the detection method. Therefore, these two different polluted lake water samples were selected as test samples, which can more effectively illustrate the applicability of this research method.

It can be seen from Table 2 that the concentrations of copper ions in Dianchi Lake and Cuihu Lake measured by this method are 0.22 μM and 0.179 μM , respectively, and the concentrations measured by ICP-MS are 0.228 μM and 0.184 μM , respectively. The difference between the results measured by these two methods is very small; similarly, the recovery rates of copper ion concentration in Dianchi Lake and Cuihu Lake samples detected by this method were 94–96% and the RSD was 4–7%; the recovery rates detected by ICP-MS were 89–97% and the RSD was 1–3%. These results show that the detection method has good reliability in practical applications.

Therefore, this method uses the above two representative polluted water samples as the actual sample detection and obtains good test results, which can show that the detection method has a wide range of applications and can be used for daily drinking water, agricultural irrigation water, domestic sewage, and other water detection.

In consideration of low cost, simple operation steps, and no need to use expensive large instruments, by comparing the detection limits of various methods for copper ions, it can be seen that the method of this study has an excellent detection limit (Table 3).

Table 3. Comparison of the LOD among different detection methods.

Detection Method	LOD	Reference
Colorimetric detection/DNAzyme	20 nM	[28]
Fluorescence detection/DNAzyme	1 nM	[36]
Colorimetric detection/DNAzyme	290 nM	[45]
Colorimetric detection/DNAzyme	1 μM	[50]
Colorimetric detection/DNAzyme	4 nM	[51]
Colorimetric detection/DNAzyme	10 μM	[59]
Colorimetric detection/DNAzyme	1 μM	[60]
Electrochemical detection/DNAzyme	30 nM	[61]
Colorimetric detection/DNAzyme	18.25 nM	This study

4. Conclusions

For the whole study, we designed a fast, sensitive, and stable DNAzyme-ligation-PCR-based visual “turn-off” colorimetric biosensor for Cu^{2+} . In this system, we combined ligation-dependent probe amplification technology with DNAzyme for the first time. Then, the special primers were designed, which include nucleic acid segments, blockers, and G-rich sequences, for performing PCR to fold into G-quadruplexes without Cu^{2+} . In this paper, some conditions of the biosensor system were optimized. The specificity and sensitivity of the system were measured under optimal conditions. The detection limit of the sensor is 18.25 nM, which is far below the regulated concentration (20 μM). Moreover, through the evaluation of different water samples, the results show that the biosensor system has good practicability and feasibility.

In addition to copper ions, this detection method can also be used for the detection of other heavy metal ions. For the detection limit and sensitivity of this study, they may be enhanced by using color enhancers to increase the G-quadruplex coloration and improved by using other signal amplification methods. At present, this method can only detect one kind of metal ion, and the realization of the detection method also involves a change in

temperature. In the subsequent research, it can be developed in the direction of multiple metal ion detection with an isothermal procedure.

Supplementary Materials: The following supporting information can be downloaded at: <https://www.mdpi.com/article/10.3390/foods12071504/s1>. Table S1: Absorbance: Optimization of copper ion cutting conditions (Figure 2C Original data); Table S2: Absorbance: Optimization of chromogenic ionic conditions (Figure 2D Original data); Table S3: Absorbance: Optimization of the concentration of H₂O₂ (Figure 2E Original data); Table S4: Absorbance: Optimization of the ratio of Cu–Enz and Cu–Su (Figure 2F Original data); Table S5: Absorbance ($\lambda = 419$ nm) under different Cu²⁺ concentrations (Figure 3B,C Original data); Table S6: Absorbance: The change of absorbance (Δ Abs) of the turn-off sensor after adding different metal ions (Figure 4A Original data); Table S7: Determination of Cu²⁺ in four different water samples using the biosensor and ICP-MS (Table 2 Original data); Figure S1: The original size of Scheme 1A; Figure S2: The original size of Scheme 1B; Figure S3: The original size of Scheme 1C.

Author Contributions: H.Z.: Methodology, data curation, writing—original draft preparation; K.D.: Methodology, data curation, writing—original draft preparation; S.X.: data analysis; Y.L.: data analysis; X.C.: software; Y.S.: Conceptualization, resources, writing—review and editing, project administration, funding acquisition; W.X.: Conceptualization, resources, writing—review and editing, project administration. All authors have read and agreed to the published version of the manuscript.

Funding: This work was supported by the National Natural Science Foundation of China (32260624) and the Yunnan Major Scientific and Technological Projects (202202AG050009).

Data Availability Statement: The data presented in this study are available on request from the corresponding author.

Conflicts of Interest: The authors declare no conflict of interest.

References

1. Hussain, I.; Afzal, S.; Ashraf, M.A.; Rasheed, R.; Saleem, M.H.; Alatawi, A.; Ameen, F.; Fahad, S. Effect of Metals or Trace Elements on Wheat Growth and Its Remediation in Contaminated Soil. *J. Plant Growth Regul.* **2022**, *26*, 1–25. [[CrossRef](#)]
2. Berni, R.; Luyckx, M.; Xu, X.; Legay, S.; Sergeant, K.; Hausman, J.F.; Lutts, S.; Cai, G.; Guerriero, G. Reactive oxygen species and heavy metal stress in plants: Impact on the cell wall and secondary metabolism. *Environ. Exp. Bot.* **2019**, *161*, 98–106. [[CrossRef](#)]
3. Khan, A.; Khan, S.; Khan, M.A.; Qamar, Z.; Waqas, M. The uptake and bioaccumulation of heavy metals by food plants, their effects on plants nutrients, and associated health risk: A review. *Environ. Sci. Pollut. Res.* **2015**, *22*, 13772–13799. [[CrossRef](#)] [[PubMed](#)]
4. Kelly, B.C.; Gobas, F.; McLachlan, M.S. Intestinal absorption and biomagnification of organic contaminants in fish, wildlife, and humans. *Environ. Toxicol. Chem.* **2004**, *23*, 2324–2336. [[CrossRef](#)]
5. Mohmand, J.; Eqani, S.; Fasola, M.; Alamdar, A.; Mustafa, I.; Ali, N.; Liu, L.P.; Peng, S.Y.; Shen, H.Q. Human exposure to toxic metals via contaminated dust: Bio-accumulation trends and their potential risk estimation. *Chemosphere* **2015**, *132*, 142–151. [[CrossRef](#)]
6. Tekaya, N.; Saiapina, O.; Ben Ouada, H.; Lagarde, F.; Ben Ouada, H.; Jaffrezic-Renault, N. Ultra-sensitive conductometric detection of pesticides based on inhibition of esterase activity in *Arthrospira platensis*. *Environ. Pollut.* **2013**, *178*, 182–188. [[CrossRef](#)]
7. Jarup, L. Hazards of heavy metal contamination. *Br. Med. Bull.* **2003**, *68*, 167–182. [[CrossRef](#)]
8. Singh, A.; Sharma, R.K.; Agrawal, M.; Marshall, F.M. Health risk assessment of heavy metals via dietary intake of foodstuffs from the wastewater irrigated site of a dry tropical area of India. *Food Chem. Toxicol.* **2010**, *48*, 611–619. [[CrossRef](#)]
9. Karube, I.; Nomura, Y.; Arikawa, Y. Biosensors for environmental control. *TrAC Trends Anal. Chem.* **1995**, *14*, 295–299. [[CrossRef](#)]
10. Bremner, I. Manifestations of copper excess. *Am. J. Clin. Nutr.* **1998**, *67*, 1069S–1073S. [[CrossRef](#)]
11. Chan, M.S.; Huang, S.D. Direct determination of cadmium and copper in seawater using a transversely heated graphite furnace atomic absorption spectrometer with Zeeman-effect background corrector. *Talanta* **2000**, *51*, 373–380. [[CrossRef](#)]
12. Santosa, S.J.; Tanaka, S.; Yamanaka, K. Inductively coupled plasma mass spectrometry for the sequential determination of trace metals in sea water after electrothermal vaporization of their dithiocarbamate complexes in methyl isobutyl ketone. *Fresenius J. Anal. Chem.* **1997**, *357*, 1127. [[CrossRef](#)]
13. Zhu, G.C.; Zhang, C.Y. Functional nucleic acid-based sensors for heavy metal ion assays. *Analyst* **2014**, *139*, 6326–6342. [[CrossRef](#)] [[PubMed](#)]
14. Zhan, S.S.; Wu, Y.G.; Luo, Y.F.; Liu, L.; He, L.; Xing, H.B.; Zhou, P. Label-free fluorescent sensor for lead ion detection based on lead(II)-stabilized G-quadruplex formation. *Anal. Biochem.* **2014**, *462*, 19–25. [[CrossRef](#)]
15. Li, W.Y.; Yang, Y.; Chen, J.; Zhang, Q.F.; Wang, Y.; Wang, F.Y.; Yu, C. Detection of lead(II) ions with a DNAzyme and isothermal strand displacement signal amplification. *Biosens. Bioelectron.* **2014**, *53*, 245–249. [[CrossRef](#)]

16. Liu, J.; Lu, Y. Rational design of “Turn-On” allosteric DNAzyme catalytic beacons for aqueous mercury ions with ultrahigh sensitivity and selectivity. *Angew. Chem. Int. Ed.* **2007**, *46*, 7587–7590. [[CrossRef](#)] [[PubMed](#)]
17. Li, T.; Dong, S.J.; Wang, E. Label-Free Colorimetric Detection of Aqueous Mercury Ion (Hg^{2+}) Using Hg^{2+} -Modulated G-Quadruplex-Based DNAzymes. *Anal. Chem.* **2009**, *81*, 2144–2149. [[CrossRef](#)] [[PubMed](#)]
18. Lang, M.J.; Li, Q.; Huang, H.M.; Yu, F.; Chen, Q.H. Highly sensitive exonuclease III-assisted fluorometric determination of silver(I) based on graphene oxide and self-hybridization of cytosine-rich ss-DNA. *Microchim. Acta* **2016**, *183*, 1659–1665. [[CrossRef](#)]
19. Li, T.; Shi, L.L.; Wang, E.K.; Dong, S.J. Silver-Ion-Mediated DNAzyme Switch for the Ultrasensitive and Selective Colorimetric Detection of Aqueous Ag^+ and Cysteine. *Chem. Eur. J.* **2009**, *15*, 3347–3350. [[CrossRef](#)] [[PubMed](#)]
20. Xu, M.D.; Gao, Z.Q.; Wei, Q.H.; Chen, G.N.; Tang, D.P. Hemin/G-quadruplex-based DNAzyme concatamers for in situ amplified impedimetric sensing of copper(II) ion coupling with DNAzyme-catalyzed precipitation strategy. *Biosens. Bioelectron.* **2015**, *74*, 1–7. [[CrossRef](#)]
21. Liu, J.; Lu, Y. A DNAzyme catalytic beacon sensor for paramagnetic Cu^{2+} ions in aqueous solution with high sensitivity and selectivity. *J. Am. Chem. Soc.* **2007**, *129*, 9838–9839. [[CrossRef](#)] [[PubMed](#)]
22. Huang, P.J.; Liu, J.W. An Ultrasensitive Light-up Cu^{2+} Biosensor Using a New DNAzyme Cleaving a Phosphorothioate-Modified Substrate. *Anal. Chem.* **2016**, *88*, 3341–3347. [[CrossRef](#)] [[PubMed](#)]
23. Moshe, M.; Elbaz, J.; Willner, I. Sensing of UO_2^{2+} and Design of Logic Gates by the Application of Supramolecular Constructs of Ion-Dependent DNAzymes. *Nano Lett.* **2009**, *9*, 1196–1200. [[CrossRef](#)] [[PubMed](#)]
24. Liu, J.W.; Brown, A.K.; Meng, X.L.; Cropek, D.M.; Istok, J.D.; Watson, D.B.; Lu, Y. A catalytic beacon sensor for uranium with parts-per-trillion sensitivity and millionfold selectivity. *Proc. Natl. Acad. Sci. USA* **2007**, *104*, 2056–2061. [[CrossRef](#)]
25. Silverman, S.K. In vitro selection, characterization, and application of deoxyribozymes that cleave RNA. *Nucleic Acids Res.* **2005**, *33*, 6151–6163. [[CrossRef](#)]
26. Gao, L.; Li, L.L.; Wang, X.L.; Wu, P.W.; Cao, Y.; Liang, B.; Li, X.; Lin, Y.W.; Lu, Y.; Guo, X.F. Graphene-DNAzyme junctions: A platform for direct metal ion detection with ultrahigh sensitivity. *Chem. Sci.* **2015**, *6*, 2469–2473. [[CrossRef](#)]
27. Li, L.; Li, B.X.; Qi, Y.Y.; Jin, Y. Label-free aptamer-based colorimetric detection of mercury ions in aqueous media using unmodified gold nanoparticles as colorimetric probe. *Anal. Bioanal. Chem.* **2009**, *393*, 2051–2057. [[CrossRef](#)]
28. Liu, J.; Lu, Y. Colorimetric Cu^{2+} detection with a ligation DNAzyme and nanoparticles. *Chem. Commun.* **2007**, *46*, 4872–4874. [[CrossRef](#)]
29. Fang, Z.Y.; Huang, J.; Lie, P.C.; Xiao, Z.; Ouyang, C.Y.; Wu, Q.; Wu, Y.X.; Liu, G.D.; Zeng, L.W. Lateral flow nucleic acid biosensor for Cu^{2+} detection in aqueous solution with high sensitivity and selectivity. *Chem. Commun.* **2010**, *46*, 9043–9045. [[CrossRef](#)]
30. Xu, X.Y.; Daniel, W.L.; Wei, W.; Mirkin, C.A. Colorimetric Cu^{2+} Detection Using DNA-Modified Gold-Nanoparticle Aggregates as Probes and Click Chemistry. *Small* **2010**, *6*, 623–626. [[CrossRef](#)]
31. Wang, F.; Orbach, R.; Willner, I. Detection of Metal Ions (Cu^{2+} , Hg^{2+}) and Cocaine by Using Ligation DNAzyme Machinery. *Chem. Eur. J.* **2012**, *18*, 16030–16036. [[CrossRef](#)] [[PubMed](#)]
32. Li, L.D.; Luo, L.; Mu, X.J.; Sun, T.Y.; Guo, L. A reagentless signal-on architecture for electronic, real-time copper sensors based on self-cleavage of DNAzymes. *Anal. Methods* **2010**, *2*, 627–630. [[CrossRef](#)]
33. Chen, Z.B.; Li, L.D.; Mu, X.J.; Zhao, H.T.; Guo, L. Electrochemical aptasensor for detection of copper based on a reagentless signal-on architecture and amplification by gold nanoparticles. *Talanta* **2011**, *85*, 730–735. [[CrossRef](#)] [[PubMed](#)]
34. Ocana, C.; Malashikhina, N.; del Valle, M.; Pavlov, V. Label-free selective impedimetric detection of Cu^{2+} ions using catalytic DNA. *Analyst* **2013**, *138*, 1995–1999. [[CrossRef](#)] [[PubMed](#)]
35. Zhang, L.L.; Zhang, Y.Y.; Wei, M.J.; Yi, Y.H.; Li, H.T.; Yao, S.Z. A label-free fluorescent molecular switch for Cu^{2+} based on metal ion-triggered DNA-cleaving DNAzyme and DNA intercalator. *New J. Chem.* **2013**, *37*, 1252–1257. [[CrossRef](#)]
36. Yin, B.C.; Zuo, P.; Huo, H.; Zhong, X.H.; Ye, B.C. DNAzyme self-assembled gold nanoparticles for determination of metal ions using fluorescence anisotropy assay. *Anal. Biochem.* **2010**, *401*, 47–52. [[CrossRef](#)]
37. Liu, M.; Zhao, H.M.; Chen, S.; Yu, H.T.; Zhang, Y.B.; Quan, X. Label-free fluorescent detection of $\text{Cu}(\text{II})$ ions based on DNA cleavage-dependent graphene-quenched DNAzymes. *Chem. Commun.* **2011**, *47*, 7749–7751. [[CrossRef](#)]
38. Zhan, S.S.; Wu, Y.G.; Wang, L.M.; Zhan, X.J.; Zhou, P. A mini-review on functional nucleic acids-based heavy metal ion detection. *Biosens. Bioelectron.* **2016**, *86*, 353–368. [[CrossRef](#)]
39. Li, H.; Huang, X.X.; Kong, D.M.; Shen, H.X.; Liu, Y. Bioelectronics, Ultrasensitive, high temperature and ionic strength variation-tolerant Cu^{2+} fluorescent sensor based on reconstructed Cu^{2+} -dependent DNAzyme/substrate complex. *Biosens. Bioelectron.* **2013**, *42*, 225–228. [[CrossRef](#)]
40. Zuo, P.; Yin, B.C.; Ye, B.C. DNAzyme-based microarray for highly sensitive determination of metal ions. *Biosens. Bioelectron.* **2009**, *25*, 935–939. [[CrossRef](#)]
41. Xiang, Y.; Lu, Y. DNA as Sensors and Imaging Agents for Metal Ions. *Inorg. Chem.* **2014**, *53*, 1925–1942. [[CrossRef](#)] [[PubMed](#)]
42. Zhang, G.Y.; Lin, W.L.; Yang, W.Q.; Lin, Z.Y.; Guo, L.H.; Qiu, B.; Chen, G.N. Logic gates for multiplexed analysis of Hg^{2+} and Ag^+ . *Analyst* **2012**, *137*, 2687–2691. [[CrossRef](#)] [[PubMed](#)]
43. Li, M.H.; Wang, Y.S.; Cao, J.X.; Chen, S.H.; Tang, X.; Zhu, X.F.; Zhu, Y.F.; Huang, Y.Q. Ultrasensitive detection of uranyl by graphene oxide-based background reduction and RCDzyme-based enzyme strand recycling signal amplification. *Biosens. Bioelectron.* **2015**, *72*, 294–299. [[CrossRef](#)] [[PubMed](#)]

44. Ge, C.C.; Chen, J.H.; Wu, W.; Fang, Z.Y.; Chen, L.B.; Liu, Q.; Wang, L.; Xing, X.R.; Zeng, L.W. An enzyme-free and label-free assay for copper(II) ion detection based on self-assembled DNA concatamers and Sybr Green I. *Analyst* **2013**, *138*, 4737–4740. [[CrossRef](#)]
45. Wang, Y.; Yang, F.; Yang, X.R. Label-free colorimetric biosensing of copper(II) ions with unimolecular self-cleaving deoxyribozymes and unmodified gold nanoparticle probes. *Nanotechnology* **2010**, *21*, 205502. [[CrossRef](#)]
46. Stefan, L.; Xu, H.J.; Gros, C.P.; Denat, F.; Monchaud, D. Harnessing Nature's Insights: Synthetic Small Molecules with Peroxidase-Mimicking DNzyme Properties. *Chem. Eur. J.* **2011**, *17*, 10857–10862. [[CrossRef](#)]
47. Kong, D.M.; Wu, J.; Wang, N.; Yang, W.; Shen, H.X. Peroxidase activity-structure relationship of the intermolecular four-stranded G-quadruplex-hemin complexes and their application in Hg²⁺ ion detection. *Talanta* **2009**, *80*, 459–465. [[CrossRef](#)]
48. Travascio, P.; Bennet, A.J.; Wang, D.Y.; Sen, D. A ribozyme and a catalytic DNA with peroxidase activity: Active sites versus cofactor-binding sites. *Chem. Biol.* **1999**, *6*, 779–787. [[CrossRef](#)]
49. Zhou, X.H.; Kong, D.M.; Shen, H.X. Ag⁺ and Cysteine Quantitation Based on G-Quadruplex-Hemin DNzymes Disruption by Ag⁺. *Anal. Chem.* **2010**, *82*, 789–793. [[CrossRef](#)]
50. Yin, B.C.; Ye, B.C.; Tan, W.H.; Wang, H.; Xie, C.C. An Allosteric Dual-DNzyme Unimolecular Probe for Colorimetric Detection of Copper(II). *J. Am. Chem. Soc.* **2009**, *131*, 14624–14625. [[CrossRef](#)]
51. Zhang, Q.; Cai, Y.; Li, H.; Kong, D.M.; Shen, H.X. Sensitive dual DNzymes-based sensors designed by grafting self-blocked G-quadruplex DNzymes to the substrates of metal ion-triggered DNA/RNA-cleaving DNzymes. *Biosens. Bioelectron.* **2012**, *38*, 331–336. [[CrossRef](#)]
52. Shang, Y.; Zhu, P.Y.; Xu, W.T.; Guo, T.X.; Tian, W.Y.; Luo, Y.B.; Huang, K.L. Single universal primer multiplex ligation-dependent probe amplification with sequencing gel electrophoresis analysis. *Anal. Biochem.* **2013**, *443*, 243–248. [[CrossRef](#)] [[PubMed](#)]
53. Kong, H.S.; Lu, Y.L.; Dong, X.; Zeng, S.Y. Quantification of the Coordination Degree between Dianchi Lake Protection and Watershed Social-Economic Development: A Scenario-Based Analysis. *Sustainability* **2021**, *13*, 116. [[CrossRef](#)]
54. Gao, L.; Yang, H.; Zhou, J.M.; Lu, J.J. Lake sediments from Dianchi Lake: A phosphorus sink or source? *Pedosphere* **2004**, *14*, 483–490.
55. Wang, R.X.; Wu, F.; Chang, Y.Y.; Yang, X.J. Waterbirds and their Habitat Utilization of Artificial Wetlands at Dianchi Lake: Implication for Waterbird Conservation in Yunnan-Guizhou Plateau Lakes. *Wetlands* **2016**, *36*, 1087–1095. [[CrossRef](#)]
56. Yin, L.; Chen, R.; Wang, X. Optimized strategies of pollution control for landscape lakes replenished with WWTP effluent based on pollutants balance analysis: A case study in Cuihu Lake in Kunming, China. *Acta Sci. Circumstantiae* **2015**, *35*, 449–455.
57. Liu, X.J.; Wang, H.L. Dianchi Lake, China: Geological formation, causes of eutrophication and recent restoration efforts. *Aquat. Ecosyst. Health Manag.* **2016**, *19*, 40–48. [[CrossRef](#)]
58. Yunzeng, C.; Hao, Y.; Feng, J.I.N.; Junjie, L.V.; Zhenke, Z.; Mingzhou, Q.I.N. Metal Pollution and Potential Ecological Risk of the Sediment in Dianchi Lake. *Soils* **2007**, *39*, 737–741.
59. Lin, H.X.; Zou, Y.; Huang, Y.S.; Chen, J.; Zhang, W.Y.; Zhuang, Z.X.; Jenkins, G.; Yang, C.J. DNzyme crosslinked hydrogel: A new platform for visual detection of metal ions. *Chem. Commun.* **2011**, *47*, 9312–9314. [[CrossRef](#)]
60. Qu, W.S.; Liu, Y.Y.; Liu, D.B.; Wang, Z.; Jiang, X.Y. Copper-Mediated Amplification Allows Readout of Immunoassays by the Naked Eye. *Angew. Chem. Int. Ed.* **2011**, *50*, 3442–3445. [[CrossRef](#)]
61. Ma, J.P.; Chen, G.Z.; Bai, W.S.; Zheng, J.B. Amplified electrochemical hydrogen peroxide sensing based on Cu-porphyrin metal-organic framework nanofilm and G-quadruplex-hemin DNzyme. *ACS Appl. Mater. Interfaces* **2020**, *12*, 58105–58112. [[CrossRef](#)] [[PubMed](#)]

Disclaimer/Publisher's Note: The statements, opinions and data contained in all publications are solely those of the individual author(s) and contributor(s) and not of MDPI and/or the editor(s). MDPI and/or the editor(s) disclaim responsibility for any injury to people or property resulting from any ideas, methods, instructions or products referred to in the content.